ARMY RESEARCH LABORATORY

Comparison Study of the BLITS and BLIRB Radiative Transport Models

David A. Ligon, Alan Wetmore, and Patti Gillespie

ARL-TR-1721-8 March 1999

Approved for public release; distribution unlimited.

The findings in this report are not to be construed as an official Department of the Army position unless so designated by other authorized documents.

Citation of manufacturer's or trade names does not constitute an official endorsement or approval of the use thereof.

Destroy this report when it is no longer needed. Do not return it to the originator.

Abstract

This report is one in a series of volumes that document the Weather and Atmospheric Visualization Effects for Simulation (WAVES) suite of models. Each volume describes an aspect of the series of models. This particular report documents a comparison of the surface-based radiative transport (RT) code Boundary Layer Illumination and Transmission for Simulation (BLITS) with the volumetric RT code for Boundary Layer Illumination and Radiation Balance (BLIRB). This comparison is made using a simple three-dimensional (3-D) scenario that consists of a homogeneous cubical cloud filled with an aerosol described by the Deirmendjian type C.1 cloud phase function. Comparisons of the two RT models are made relative to results from two separate but consistent Monte Carlo models. For this simple scenario, BLIRB was determined to perform better than BLITS for the complete range of optical depths used. The BLITS model failed to accurately describe the radiant intensity of the scattering in the atmosphere at low optical depths.

Contents

Figures

Tables

1. Introduction

This report is one in a series of U.S. Army Research Laboratory (ARL) reports (ARL-TR-1721-1–8) that documents the WAVES (Weather and Atmospheric Visualization Effects for Simulation) suite of models.* A number of experimental and computational validations have been conducted for WAVES [1–7]. These previous studies contribute to the model evaluation of WAVES.

Specifically, this report documents a comparison between the Boundary Layer Illumination and Radiation Balance (BLIRB) radiative transport (RT) model and the Boundary Layer Illumination and Transmission for Simulation (BLITS) RT model using a standard scenario first used by McKee and Cox [8,9]. This comparison was deemed necessary for two reasons. First, due to continuing work on the BLIRB 8-stream RT model and changes to the aerosol phase function database (PFNDAT) used by BLIRB, it was necessary to redo the previous tests of BLIRB done by Zardecki [3,10–12]. Second, in Tofsted [13], radiative transfer through dense clouds by BLIRB was cited as problematic. Previous computational comparisons were made by Zardecki [10] to a McKee and Cox [8] Monte Carlo calculation and by Wells [14] with his order-of-scattering Monte Carlo model. These comparisons indicated that for dense media, i.e., thick clouds, the grid spacing of the calculations should be decreased and the number of streams used in the RT calculations by BLIRB should be increased. More recently, experimental data have been compared to BLIRB calculations by Gillespie et al [4], Mozer et al [5], and Wetmore et al [6]. The Gillespie comparison indicated that the blurring effect of turbulence was probably underestimated and the contrast reduction due to scattering and attenuation was slightly excessive. The Mozer comparison indicates that the order of magnitude of contrast reduction is correct. In this report, we will focus on the simple, homogenous cloud scenario described by McKee and Cox [8] and do a computational comparison.

For the McKee and Cox scenario, the modeled volume is a 5-km cube containing a homogenous Deirmendjian type C.1 cloud (see fig. 1).

*The appendix of this report describes the volumes in this series.

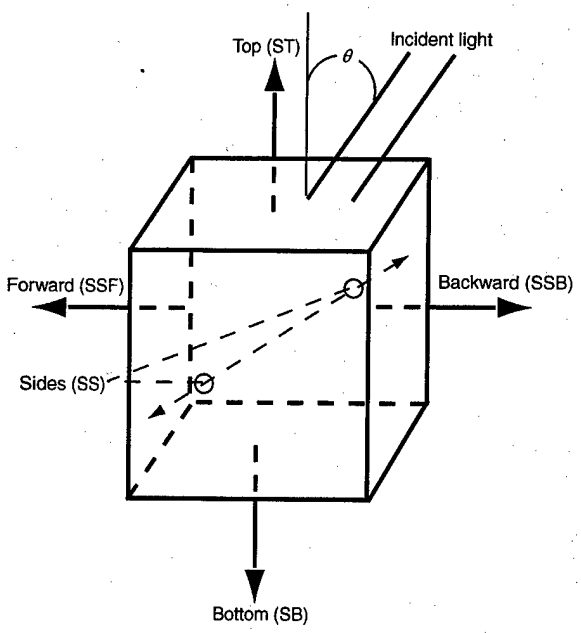

Figure 1. Description of geometry used for comparison study. For abnormal solar incidence, only faces labeled SSB and ST are directly illuminated.

This cloud type models cumulus clouds and is described by a size distribution given by

$$\frac{\partial n}{\partial r} = 2.373 r^6 e^{-1.5r} \quad . \tag{1}$$

Integrating equation (1) over all particle radii gives a number density of 100 cm^{-3}, which results in a volume scattering coefficient of 16.33 km^{-1}. A graph of the Deirmendjian phase function, calculated from the Mie theory using equation (1), is presented in figure 2. The scattering phase function is characterized by a very strong forward-scattering peak with 50 percent of the scattered radiation contained in the first 6° around the forward direction. For the McKee and Cox scenario, the scattering is chosen to be conservative, i.e., no absorption. For an aerosol composed of water at visible wavelengths, this is a good approximation. Calculations were made for an incident wavelength of 0.45 μm and total optical depths of 4.9, 10.0, 15.0, 25.0, 51.8, and 73.5. The calculations were made for solar incident angles of 0°, 30°, and 60°. The total number of photons exiting each of the six faces (see fig. 1) was used to compare the different methods. For both BLIRB and BLITS an 8-stream model was used and the volume was discretized using 25^3 cubical cells (200-m resolution).

The results of the McKee and Cox Monte Carlo simulation are used as the accepted results for comparing the BLIRB and BLITS models. However, for direct comparison of individual faces of the cloud volume, a different

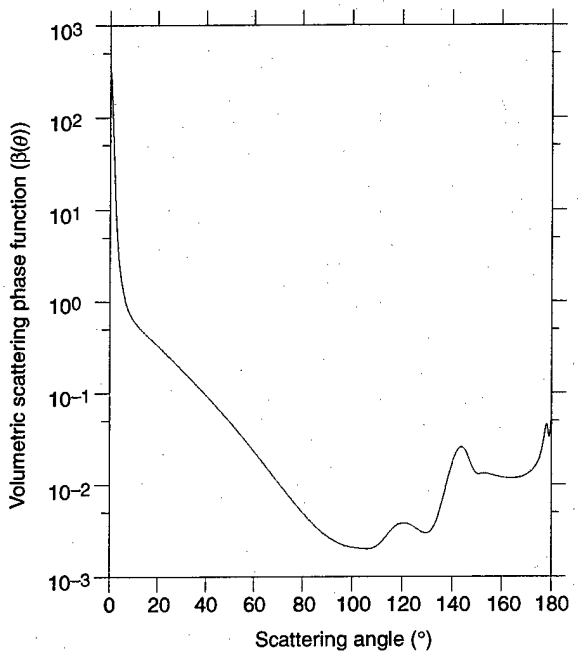

Figure 2. Volumetric scattering phase function for a Deirmendjian type C.1 cloud for wavelength of $\lambda = 0.45$ μm.

Monte Carlo simulation was used. This was necessary, as the published results of McKee and Cox did not include a breakdown of the flux that exits each face of the volume for every optical depth used.

The AGGIE (A Generalized Geometry Irradiance Estimator) Monte Carlo code written by Michael Wells [14] was used in this study to compare the results for the fluxes that were exiting each of the six faces of the volume. By comparing resulting fluxes leaving the bottom, top, and sum total of the side faces from AGGIE with those from the McKee and Cox study, we can show that AGGIE is consistent with their results. From this we infer that the AGGIE results for each face are correct.

During this comparison, a few important discoveries were made regarding previous comparisons. First, the results from the Monte Carlo models were not scaled correctly. The McKee and Cox scenario is specifically conservative. The conservative assumption means that there is no absorption from the aerosol. However, the results for the fraction of energy exiting each of the faces, as taken from the findings of McKee and Cox [8] and Wells [14], show that a scale term is needed to account for missing energy. In the case of McKee and Cox, these scale terms were needed for the smaller optical depths for solar zenith angle incidence of 30° and 60°. The AGGIE results were not scaled correctly at large optical depths, which is due primarily to incomplete sampling. Second, the phase function representing the Deirmendjian type C.1 cloud used by BLIRB in previous

comparisons was inadequate. This phase function did not have as sharp a forward-scattering lobe as the phase function used in this comparison.

We begin with a brief background discussion of the different methodologies used in this comparison study. We first describe the Monte Carlo methods employed in the McKee and Cox and AGGIE simulations and then describe the discrete ordinates method (DOM) as it applies to both the BLIRB and BLITS models.

2. Background

2.1 Monte Carlo Methods

2.1.1 McKee and Cox

The Monte Carlo analysis of McKee and Cox [8,9] has been considered the standard by which to compare three-dimensional (3-D) RT modeling. The Monte Carlo technique used in their investigation was a direct simulation of the scattering processes in the atmosphere. In this technique, for each individual photon entering the scattering volume, the trajectory is tracked through a series of scattering events until the photon either exits the volume or is absorbed within the volume. The distance traveled between scattering events is found from the probability of a photon traveling the same distance. The probability PR is related to the optical depth by

$$PR = e^{-\tau} = \exp\left(-\int_0^s \beta ds\right) \quad , \tag{2}$$

where β is the volume scattering coefficient and s is the distance traveled. In the simulation, a random number RN is chosen for the probability PR, and the distance to a scattering event is determined by the upper limit of integration of

$$-\int_0^s \beta ds = \tau = -\ln(1 - RN) \quad . \tag{3}$$

For a homogeneous scattering volume, β is constant, so equation (3) simply reduces to

$$s = -\frac{1}{\beta}\ln(1 - RN) \quad . \tag{4}$$

To determine the scattering angle, the single scattering phase function $P(\alpha)$, where α is the scattering angle measured from the direction of propagation before the collision to the direction after the collision, is sampled similarly to the steps above. The probability of a photon being scattered between 0 and α is given by

$$PP(\alpha) = 2\pi \int_0^\alpha P(\alpha)\, d(\cos\alpha) \quad . \tag{5}$$

The scattering angle α is determined by choosing a random number for $PP(\alpha)$ and solving equation (5) for the upper limit of integration. The second angle needed to define the direction of propagation before the collision γ is a uniformly distributed rotation about the direction of propagation before the collision and is picked randomly from between 0 and 2π. McKee and Cox's analysis specifically treated the aerosol as nonabsorbing. A more complete description of the method and results can be found in the original paper [8].

The data used in our comparison were taken from a digitization of McKee and Cox's graphs [8]. During this digitization, we determined that the total fraction of light scattered from the six faces of the cubical cloud did not sum to unity for the 30° and 60° solar incidence. This departure was largest in the smaller optical depths used. We were unable to account for this discrepancy in McKee and Cox's method. As our scenarios were designed to simulate a nonabsorbing cloud, we decided to rescale the results for each optical depth, such that the total of the fractions of the energy leaving each face would equal 1. At no point was this total fraction less than 0.88. The rescaled data are summarized in table 1.

2.1.2 AGGIE

We used the AGGIE Monte Carlo code written by Wells [14] in this study to compare the results for the fluxes exiting each of the six faces of the volume. This was necessary as the published results of McKee and Cox did not include a breakdown of the flux exiting each side of the volume for every optical depth used. By comparing resulting fluxes leaving the bottom, top, and sum total of the side faces from AGGIE with those from the McKee and Cox study, we can show that AGGIE is consistent with the McKee and Cox results. From this we inferred that the AGGIE results for each face were correct and used these to compare the BLIRB and BLITS

Table 1. Fraction of incident energy exiting faces from McKee and Cox model.

	Solar incidence angle								
	$\theta = 0°$			$\theta = 30°$			$\theta = 60°$		
Optical depth	Sides	ST	SB	Sides	ST	SB	Sides	ST	SB
4.9	0.51	0.07	0.42	0.55	0.05	0.40	0.62	0.07	0.31
10.0	0.66	0.12	0.22	0.63	0.09	0.28	0.64	0.10	0.26
15.0	0.70	0.18	0.12	0.65	0.14	0.21	0.64	0.14	0.23
25.0	0.67	0.26	0.07	0.66	0.18	0.16	0.63	0.19	0.18
51.8	0.57	0.40	0.03	0.62	0.29	0.09	0.63	0.24	0.13
73.5	0.49	0.49	0.02	0.58	0.35	0.07	0.62	0.28	0.10

ST = top, SB = bottom

results more thoroughly. AGGIE calculations were originally done to evaluate BLIRB for 3-D cloud scenarios that were more complex than those of McKee and Cox.

Historically, the AGGIE code has been used for neutron transport and RT studies. The Monte Carlo technique used in AGGIE is essentially an order-of-scattering approach. This approach only calculates the scattering due to a finite (approximately 60) number of orders (the scattering events). The technique follows closely that of McKee and Cox: it creates a photon and follows it along a randomly generated path, but it maintains the location of all the scattering events in a trajectory history for later use. Each photon trajectory starts at a random point on the top surface of the scattering volume, moving in alignment with the solar zenith angle. After the scattering trajectories are calculated, they are used in the calculation of the fluxes that exit each face of the scattering volume. Each scattering point on a trajectory is used as a source location of candidate photons to be tested against the probability of being scattered onto a trajectory that would exit the volume without further collisions. These probabilities are combined with the probability of arriving at the particular point on the trajectory to calculate the photon fluxes that exit each face of the scattering volume.

Although this method is more efficient than McKee and Cox's, it is not as accurate a representation of multiple scattering as the more rigorous direct Monte Carlo simulation of McKee and Cox. However, for the scenario tested here, enough scattering orders were retained to adequately simulate the RT. Wells' results also required rescaling due to incomplete sampling of the scattering probability (due to the finite number of scattering orders). The rescale terms were most noticeable for the large optical depths, as should be expected for incomplete sampling. The rescaled AGGIE data are summarized in tables 2, 5, and 6.

Table 2. Fraction of incident energy exiting faces from AGGIE model.

	Solar incidence angle								
	$\theta = 0°$			$\theta = 30°$			$\theta = 60°$		
Optical depth	Sides	ST	SB	Sides	ST	SB	Sides	ST	SB
4.9	0.49	0.07	0.44	0.55	0.05	0.40	0.63	0.05	0.32
10.0	0.66	0.12	0.22	0.63	0.09	0.28	0.63	0.10	0.27
15.0	0.70	0.17	0.13	0.65	0.13	0.22	0.63	0.12	0.25
25.0	0.69	0.25	0.06	0.66	0.19	0.15	0.63	0.18	0.19
51.8	0.58	0.41	0.01	0.62	0.29	0.09	0.62	0.25	0.13
73.5	0.49	0.50	0.01	0.59	0.34	0.07	0.63	0.27	0.10

ST = top, SB = bottom

2.2 Discrete Ordinates Method

The DOM employed by the BLIRB and BLITS models uses an iterative scheme to solve the 3-D RT equation. For atmospheric simulations, the time-independent equation of RT is explicitly written in a form that does not contain the wavelength dependence:

$$\left[\widehat{\Omega}\cdot\nabla+\sigma\left(\vec{r}\right)\right]I\left(\vec{r},\widehat{\Omega}\right)=\int\widetilde{\sigma}_s\left(\vec{r},\widehat{\Omega}\cdot\widehat{\Omega}'\right)I\left(\vec{r},\widehat{\Omega}'\right)d\widehat{\Omega}'+s\left(\vec{r},\widehat{\Omega}\right). \quad (6)$$

In equation (6), I is the specific intensity (radiance distribution function) defined such that $Id\widehat{\Omega}$ is the flux density of radiant energy about the point $\vec{r}$ in the infinitesimal solid angle $d\widehat{\Omega}$, σ is the space-dependent volume extinction coefficient, $\widetilde{\sigma}_s$ is the differential volume scattering coefficient, and s is the source term for sources independent of I (such as flares, thermal emission, etc).

Standard DOMs solve the equation of RT, equation (6), using an iterative-series solution referred to as iteration on the source. The method relies on an iterative approximation to the right-hand side of equation (6) that results in a convergent procedure for the radiance distribution function. The iteration procedure is given by

$$\left[\widehat{\Omega}\cdot\nabla+\sigma\left(\vec{r}\right)\right]I^{k+1}\left(\vec{r},\widehat{\Omega}\right)=q^k\left(\vec{r},\widehat{\Omega}\right), \quad (7)$$

where the scattering source is given as

$$q^k\left(\vec{r},\widehat{\Omega}\right)=\int\widetilde{\sigma}_s\left(\vec{r},\widehat{\Omega}\cdot\widehat{\Omega}'\right)I^k\left(\vec{r},\widehat{\Omega}'\right)d\widehat{\Omega}'+s\left(\vec{r},\widehat{\Omega}\right), \quad (8)$$

where k is the iteration index. The method for solution of equation (7) consists of two parts: one, characterization and solution for the angular variables and two, solution on the spatial variables.

The DOM evolves from the quadrature selected for carrying out the angular integration of equation (8). First, the differential volume scattering coefficient $\widetilde{\sigma}_s$ is represented by a finite Legendre polynomial expansion of order L:

$$\widetilde{\sigma}_s\left(\vec{r},\widehat{\Omega}\cdot\widehat{\Omega}'\right)=\sum_{l=0}^{L}\frac{2l+1}{4\pi}\sigma_s^l\left(\vec{r}\right)P_l\left(\widehat{\Omega}\cdot\widehat{\Omega}'\right). \quad (9)$$

By selecting the proper quadrature (integration scheme), the integral of equation (8) can be written as a simple series of finite order. In this study, both BLIRB and BLITS used S_2 quadrature, which consists of eight streams defined by the directions $\widehat{\Omega}_x=\widehat{\Omega}_y=\widehat{\Omega}_z=\pm\frac{1}{\sqrt{3}}$. Selecting this quadrature forces the Legendre expansion of $\widetilde{\sigma}_s$, equation (9), to be of the order $L=2$.

The spatial portion of equation (7) is solved using a standard finite-difference method. The spacial differencing is accomplished by dividing the x, y, z-domain into cells bounded by $x_{\frac{1}{2}}, x_{\frac{3}{2}}, ..., x_{\frac{I}{2}}$; $y_{\frac{1}{2}}, y_{\frac{3}{2}}, ..., y_{\frac{J}{2}}$; and $z_{\frac{1}{2}}, z_{\frac{3}{2}}, ..., z_{\frac{K}{2}}$. The cell centers are then located at x_i, y_j, and z_k . The final form of the transfer equation, discrete in both directions and space, is

$$\frac{\mu_n}{\Delta x_i}\left(I_{n,i+\frac{1}{2},jk} - I_{n,i-\frac{1}{2},jk}\right) + \frac{\eta_n}{\Delta y_j}\left(I_{ni,j+\frac{1}{2},k} - I_{ni,j-\frac{1}{2},k}\right) + \frac{\xi_n}{\Delta z_k}\left(I_{nij,k+\frac{1}{2}} - I_{nij,k-\frac{1}{2}}\right) + \sigma_{ijk} I_{nijk} = Q_{nijk} \quad , \tag{10}$$

where μ_n, η_n, and ξ_n are the direction cosines for the nth stream. This equation is supplemented by the diamond-difference relationships that relate the directional radiance at the center of the scattering cell with the face-centered directional radiance:

$$\begin{aligned} I_{nijk} &= \frac{1}{2}\left(I_{n,i+\frac{1}{2},jk} + I_{n,i-\frac{1}{2},jk}\right), \\ I_{nijk} &= \frac{1}{2}\left(I_{ni,j+\frac{1}{2},k} + I_{ni,j-\frac{1}{2},k}\right), \quad \text{and} \\ I_{nijk} &= \frac{1}{2}\left(I_{nij,k+\frac{1}{2}} + I_{nij,k-\frac{1}{2}}\right). \end{aligned} \tag{11}$$

Equation (10), together with the diamond-difference relationships, allows for the solution of the radiance distribution at each grid point along each discrete ordinate direction. A much more complete description of DOM and its implementation in both the BLIRB and BLITS models can be found in Zardecki [10] and Tofsted [13].

2.2.1 BLIRB

The BLIRB model is a volumetric-based, DOM RT model that computes the general illumination fields in a specific volume in the spectral range between 0.35 and 40.0 μm. BLIRB was developed for near-earth scenarios and deals with regions up to 20 km^2 from the ground to either 5 or 12 km above ground level (AGL). This allows most cloud phenomena to be explored. For example, for each 3-D grid, BLIRB computes several physical quantities: the directly transmitted solar (or lunar) radiance or flux, the directional radiances—the streams of radiances based on the Legendre expansion of the DOM RT solution, and the extinction and scattering of electromagnetic radiation. Typical spatial resolutions are on the order of 250 m. BLIRB is the RT module in the WAVES suite of models. The current version of BLIRB incorporates a generalized N-stream DOM; however, our comparison study was performed using the hard-coded 8-stream model that was used in previous comparison studies [3,10].

2.2.2 BLITS

The BLITS model was written by Tofsted and O'Brien of ARL [13]. BLITS was primarily designed for rapid simulation of 3-D natural clouds. The BLITS code, provided by Tofsted, was hard-coded for the Deirmendjian type C.1 cloud. For this comparison, both BLIRB and BLITS were run using the 8-stream model. BLITS contains many of the same elements as BLIRB but performs its calculation for the diffuse light using a surface-based DOM. BLITS also uses a phenomenological technique to extend the method to treat large optical depth conditions using surface-like scattering and absorption. A more complete description of BLITS is in Tofsted and O'Brien [13].

3. Results

Tables 1 through 4 summarize the results from the McKee and Cox, AGGIE, BLIRB, and BLITS models, respectively. The data presented are the total fractions of energy exiting the top, bottom and four side faces of the cubical volume. Tables 5 and 6 present a breakdown of the fractions leaving the faces labeled SSF (forward), SSB (backward) and SS (side) for solar incidence of 30° and 60°, respectively (see fig. 1).

To compare individual faces, we will first show that the AGGIE results are consistent with the McKee and Cox results and then compare BLIRB and BLITS with AGGIE. This step is necessary because McKee and Cox did not present data for individual faces. We have adopted a 10-percent accuracy rule as compared to the results of the AGGIE model. As a general note, when the total energy leaving a face drops below 5 percent of the total energy, the accuracy of the results become suspect. This is in part due to the convergence criterion used in each of the models as well as the standard statistical sampling noise present in any Monte Carlo simulation.

3.1 Normal Incidence

The results for normal solar incidence are plotted in figure 3. The results from the two Monte Carlo models are consistent with each other for the fraction of incident energy exiting the side, top, and bottom faces of the volume. For optical depths (OD) larger than about 50, the AGGIE model slightly underestimates the fraction exiting the bottom face of the volume

Table 3. Fraction of incident energy exiting faces from BLIRB model.

	Solar incidence angle								
	$\theta = 0°$			$\theta = 30°$			$\theta = 60°$		
Optical depth	Sides	ST	SB	Sides	ST	SB	Sides	ST	SB
4.9	0.51	0.05	0.44	0.57	0.05	0.38	0.61	0.07	0.32
10.0	0.69	0.11	0.20	0.65	0.09	0.26	0.61	0.12	0.27
15.0	0.73	0.17	0.10	0.67	0.13	0.20	0.62	0.14	0.24
25.0	0.70	0.26	0.04	0.66	0.20	0.14	0.62	0.19	0.19
51.8	0.56	0.43	0.01	0.60	0.31	0.09	0.63	0.23	0.14
73.5	0.48	0.52	0.00	0.57	0.36	0.07	0.64	0.25	0.11

ST = top, SB = bottom

Table 4. Fraction of incident energy exiting faces from BLITS model.

	Solar incidence angle								
	$\theta = 0°$			$\theta = 30°$			$\theta = 60°$		
Optical depth	Sides	ST	SB	Sides	ST	SB	Sides	ST	SB
4.9	0.70	0.03	0.27	0.65	0.04	0.31	0.60	0.09	0.31
10.0	0.81	0.10	0.09	0.70	0.09	0.21	0.61	0.13	0.26
15.0	0.79	0.16	0.05	0.70	0.13	0.17	0.63	0.15	0.22
25.0	0.73	0.25	0.02	0.68	0.19	0.13	0.62	0.20	0.18
51.8	0.59	0.40	0.01	0.63	0.29	0.08	0.62	0.25	0.13
73.5	0.52	0.47	0.01	0.59	0.34	0.07	0.62	0.27	0.10

ST = top, SB = bottom

Table 5. Breakdown of side faces for solar incidence of 30° for three models.

	AGGIE			BLIRB			BLITS		
Optical depth	SSF	SSB	SS	SSF	SSB	SS	SSF	SSB	SS
4.9	0.315	0.054	0.092	0.317	0.069	0.094	0.310	0.085	0.129
10.0	0.267	0.104	0.128	0.272	0.115	0.130	0.261	0.132	0.156
15.0	0.230	0.139	0.141	0.238	0.146	0.141	0.228	0.162	0.158
25.0	0.189	0.184	0.144	0.193	0.185	0.141	0.185	0.199	0.150
51.8	0.132	0.245	0.121	0.135	0.232	0.119	0.132	0.247	0.125
73.5	0.102	0.273	0.105	0.113	0.247	0.103	0.111	0.265	0.112

SSF = forward side, SSB = backward side, SS = left and right sides

and overestimates the fraction exiting the top face. However, this discrepancy between the two methods is well within the error limits for either model.

The results from BLIRB compare favorably with the McKee and Cox results over the complete range of optical depths used. For the fraction exiting the side faces, BLIRB is at most 4 percent off the McKee and Cox results and has an average error of 1.3 percent over the entire range. For the top face, BLIRB generally overestimated the fraction exiting the face for increasing optical depth. For $OD = 73.5$, BLIRB overestimates by roughly 7 percent and had an average error rate of 4 percent over the entire range. For the fraction exiting the bottom, BLIRB's results were consistently lower than the McKee and Cox results for increasing optical depth. This is due primarily to the approximations made in the algorithm (diamond-difference [10]).

The results from BLITS diverge markedly from the McKee and Cox results for the side and bottom faces for $OD < 50$. For example, BLITS consistently overestimated the fraction exiting the side faces. It had an average percentage difference of 15 percent from the McKee and Cox results with a maximum difference of 37 percent for $OD = 4.9$. For the

Table 6. Breakdown of side faces for solar incidence of 60° for three models.

	AGGIE			BLIRB			BLITS		
Optical depth	SSF	SSB	SS	SSF	SSB	SS	SSF	SSB	SS
4.9	0.397	0.050	0.092	0.380	0.047	0.094	0.308	0.042	0.129
10.0	0.284	0.090	0.128	0.261	0.093	0.129	0.208	0.092	0.156
15.0	0.180	0.143	0.155	0.212	0.132	0.141	0.166	0.133	0.158
25.0	0.155	0.186	0.142	0.143	0.195	0.142	0.125	0.195	0.145
51.8	0.087	0.291	0.122	0.087	0.307	0.119	0.084	0.291	0.125
73.5	0.069	0.345	0.105	0.069	0.364	0.103	0.068	0.337	0.112

SSF = forward side, SSB = backward side, SS = left and right sides

Figure 3. Comparison results for several models for normal solar incidence.

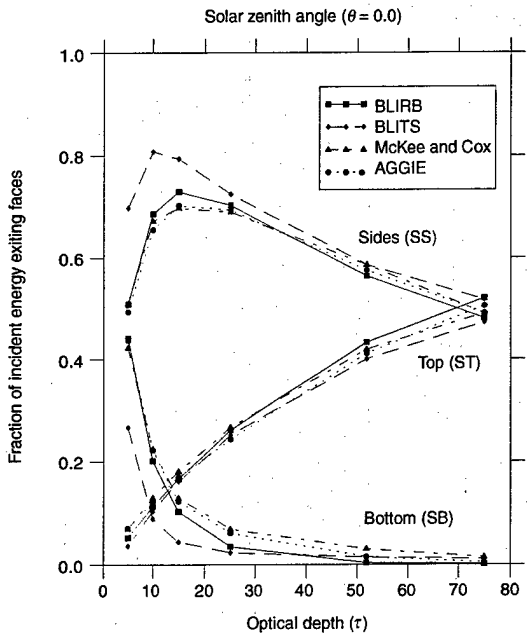

bottom face, BLITS underestimated the fraction exiting the face. As with the sides, it had an average percentage difference of 15 percent from the McKee and Cox results with a maximum difference of 35 percent for $OD = 4.9$. Toward the higher optical depths ($\gtrsim 50$) BLITS appears to approach the Monte Carlo results. For the top face, BLITS appears to be consistent with the McKee and Cox results with a tendency of slightly underestimating the exiting fraction for increasing optical depths. This is probably a result of the finite Legendre expansion of the phase function [11].

Figure 4 presents the percentage difference of BLIRB and BLITS from the AGGIE results as a function of optical depth. From figure 3, we see that for the top face, for $OD = 4.9$, the total energy leaving the face is on the

Figure 4. Percentage difference from AGGIE results for several models for normal solar incidence.

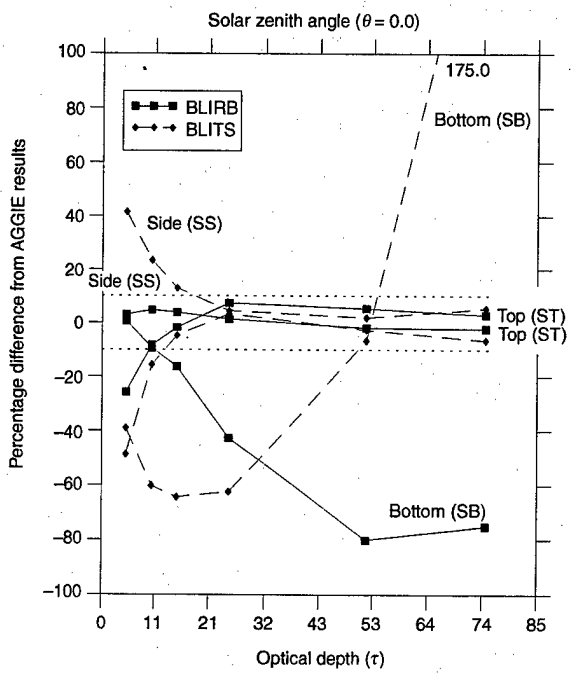

Note: The large percentage differences for the face labeled SB should be viewed with some skepticism as the total flux exiting the bottom face is very small.

order of 5 percent. For the reasons described above, the results for this data point should be viewed with some skepticism. For the same reason, the results for the bottom face, for $OD \gtrsim 30$, should also be viewed with care. As can be seen in figure 4, for the top and side faces, BLIRB fell well within the 10-percent accuracy criterion, while BLITS fell outside the criterion for the lower optical depths. For the bottom face, BLIRB fell within the acceptance criterion for only the first two data points. BLITS, however, was consistently outside the 10-percent limit for the entire optical depth considered.

Also, for normal incidence, we have a convenient consistency check. Namely, symmetry dictates that the flux from each of the four sides be equal. Both BLIRB and BLITS results were consistent in this regard.

3.2 Solar Incidence at 30°

Figure 5 shows the results for a solar incidence angle of 30°. As can be seen, the Monte Carlo results are again consistent for the incident energy exiting the faces of the volume. In general, BLIRB results compare well to the McKee and Cox results for the full range of optical depths used. Also, as before, BLITS performed poorly toward the smaller optical depths.

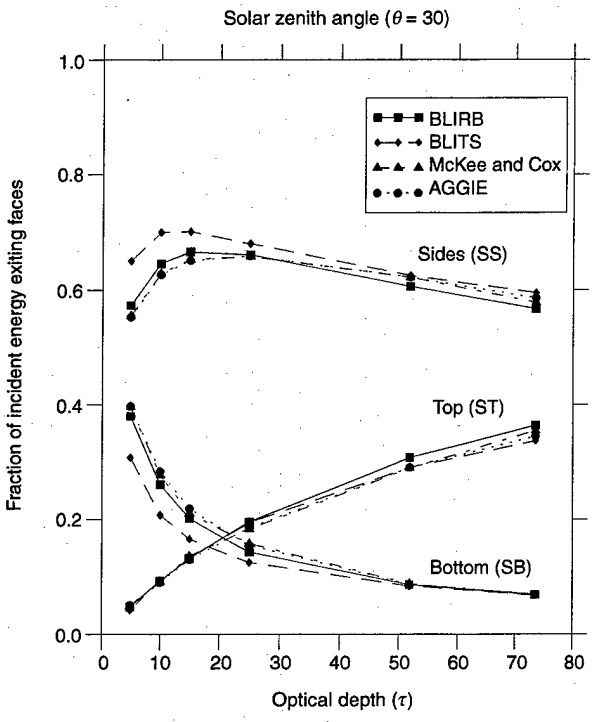

Figure 5. Comparison results for several models for solar incidence angle of 30°.

To better see the results from the side faces, figures 6 and 7 show the breakdown of the fraction of incident energy exiting the side, top, and bottom faces, as defined in figure 1. From figure 6, we see that for radiation exiting from the forward side (SSF), both BLIRB and BLITS were accurate over the full range of optical depths. For the backward face (SSB), BLIRB shows a tendency to underestimate the energy exiting the face. BLITS appears to compare favorably with McKee and Cox for the backward face. For the side faces (SS), BLIRB was consistent over all optical depths, while BLITS again shows a tendency to overestimate the exiting energy for the side faces for small optical depths. Figure 7 restates the results from figure 5 for the top and bottom faces.

Figures 8 and 9 show the comparison of BLIRB and BLITS with the AGGIE results for the side, top, and bottom faces, respectively. From figures 6 and 7, we see that more than 5 percent of the total energy was leaving every face, so we expect that all the data points should be considered important. For the side faces (labeled SSF, SSB, and SS) (see fig. 6), BLIRB met the 10-percent accuracy criterion for all the faces except the face labeled SSB at $OD = 4.9$. BLITS, however, was considerably outside the 10-percent limit for both the faces labeled SS and SSB for $OD < 20.0$. Figure 7 shows the comparison for the top and bottom faces. Again, BLIRB was inside the 10-percent criterion for both

the faces over all the optical depths investigated. BLITS was outside the 10-percent criterion for the face SB for $OD < 40.0$. It also was outside the 10-percent interval for the face ST at $OD = 4.9$.

As before, symmetry dictates that the flux leaving the two sides labeled SS be equal. Again, both BLIRB and BLITS satisfied this check.

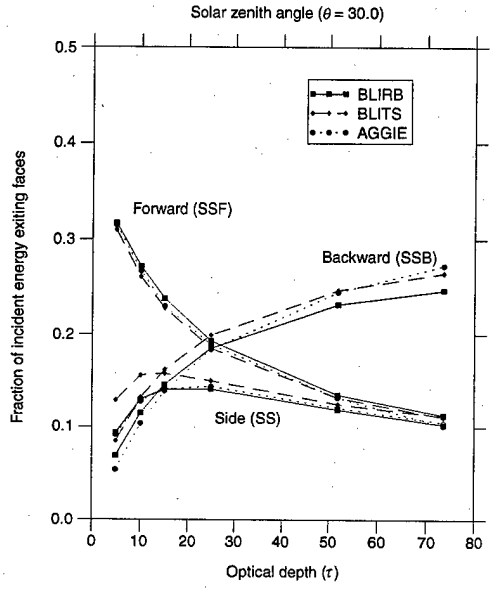

Figure 6. Breakdown of forward, backward, and side faces for solar incidence of 30°.

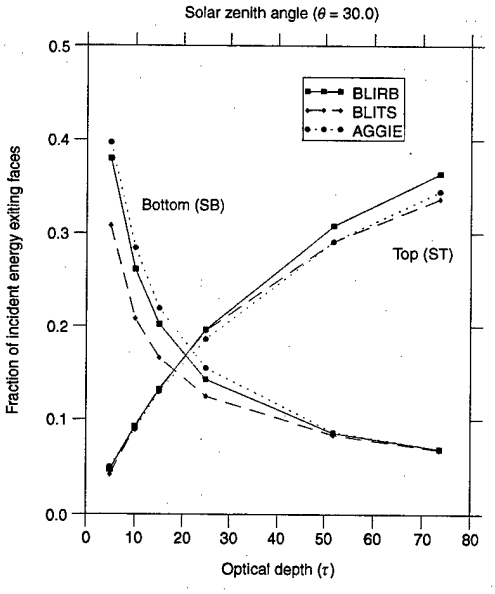

Figure 7. Breakdown of results for calculations using several models for top and bottom faces for solar incidence of 30°.

Figure 8. Percentage difference from AGGIE results for solar incidence of 30° for forward, backward, and side faces.

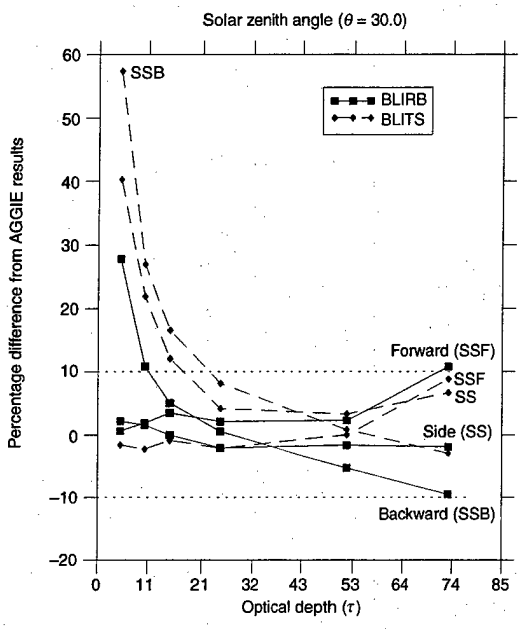

Figure 9. Percentage difference from AGGIE results for solar incidence of 30° for top and bottom faces.

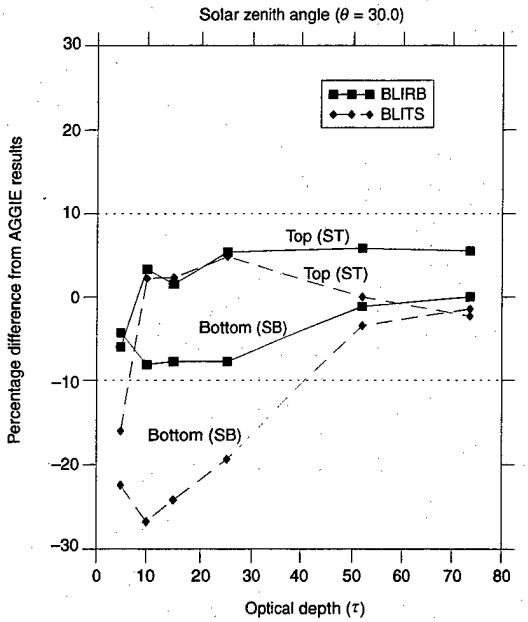

3.3 Solar Incidence at 60°

The results for a solar incident angle of 60° are shown in figure 10. At first glance, both BLIRB and BLITS appear to be in good agreement with the McKee and Cox results. Upon closer inspection of the side faces, however, this is not the case. Figure 11 shows the breakdown for the side faces. BLIRB results are similar to the Monte Carlo results for the forward and side faces and are overestimated for the backward face for increasing optical depth. The BLITS model again has difficulty with the smaller optical depths for both the forward and side faces but tracks the Monte Carlo results for the backward face. Figure 12 shows the breakdown for the top and bottom faces. For these faces, both BLIRB and BLITS are consistent with the Monte Carlo results. BLIRB does have the tendency to underestimate the exiting fraction of energy with increasing optical depth for the top face.

We can use symmetry again as a consistency check. The scenario with solar incidence at 30° should be equivalent to the scenario at 60° solar incidence with a suitable rotation of the sides. With the use of symmetry, the flux from faces ST, SB, SSF, and SSB for 30° incidence should be equivalent with the respective faces SSB, SSF, SB, and ST for 60° incidence. As can be seen in figures 6, 7, 11, and 12, both BLIRB and BLITS were consistent at both angles of incidence. Also, as at 30° incidence, the sides labeled SS should be equal. Both BLIRB and BLITS satisfied this symmetry check.

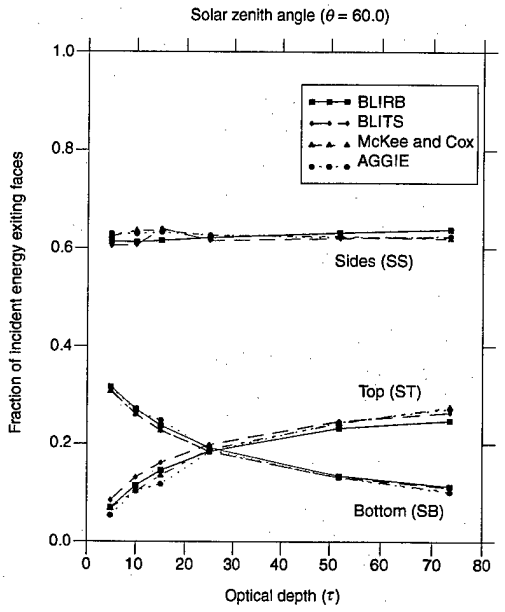

Figure 10. Comparison of results for several models for top, bottom, and side faces for solar incidence angle of 60°.

Figure 11. Breakdown of results for several models for forward, backward, and side faces for solar incidence of 60°.

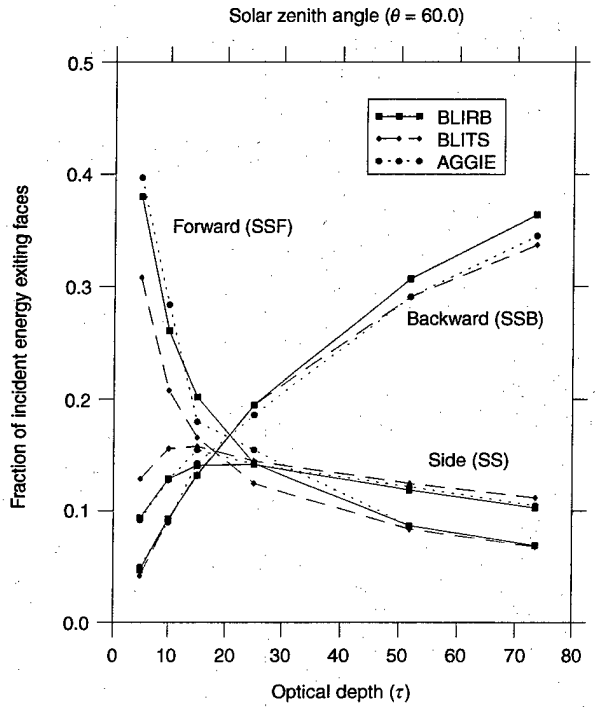

Figure 12. Breakdown of results for several models for top and bottom faces for solar incidence of 60°.

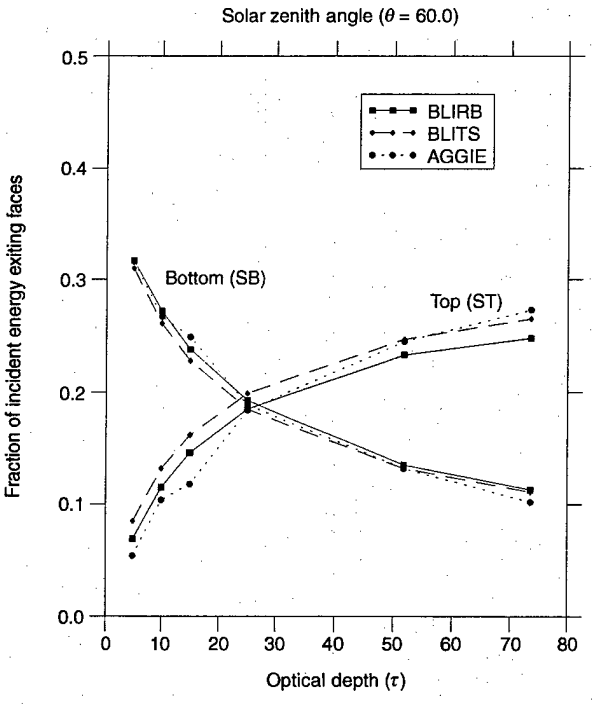

4. Conclusion

Under this comparison study, the BLIRB model clearly performed better than the BLITS model for the McKee and Cox scenario investigated. The results clearly show that BLITS fails toward the smaller optical depths ($\tau < 30$). This may be due to an inherent optimization of the BLITS algorithm for high optical depths. While the results of BLITS for high optical depths approached the Monte Carlo results, its general characteristics at lower optical depths become problematic for its use in general problems involving complex 3-D atmospheres. This being said, its performance at very high optical depths, not tested here, may warrant its use for cloud visualizations in which the optical depth can be considerably higher than in this study ($\gtrsim 300$). For these optical depths, we expect the performance of BLIRB to drop off markedly due to the approximations made in the algorithm (diamond-difference).

Using the recalculated phase function for the Deirmendjian type C.1 cloud, BLIRB performed better than in previous tests [10,14] using this scenario. Further testing should be conducted to determine BLIRB's performance using higher quadrature (i.e., a 16- or 24-stream DOM); however, we expect that BLIRB's performance will only improve from these current results. Also, although not a considerable difference was made by rescaling the McKee and Cox and AGGIE results, we are now confident that the comparisons were made using the same quantities. Further comparison could be made to determine the performance at larger optical depths. Problems with larger optical depths are expected to be overcome by decreasing the grid size or increasing the number of streams. Although computational time was not included specifically in this comparison because of the extreme difference in the amount of background calculations performed in BLIRB versus BLITS, the two codes appeared to run in approximately the same time.

References

1. Michael B. Wells, *Monte Carlo Code for Evaluating the Boundary Layer Illumination and Radiation Balance Model (BLIRB)*, U.S. Army Research Laboratory, ARL-CR-193 (1995).

2. Michael B. Wells, *Monte Carlo Code for Evaluating the Boundary Layer Illumination and Radiation Balance Model (BLIRB)*, U.S. Army Research Laboratory, ARL-CR-203 (1996).

3. Andrew Zardecki, *Testing and Evaluation of the Boundary Layer Illumination Radiation Balance Model: BLIRB*, STC technical report 6222, final report for DAAL03-91-C-0034, Las Cruces, NM (March 1992).

4. Patti Gillespie, J. Michael Rollins, and David Tofsted, "Evaluation of WAVES Using Image Statistics," *Proceedings of the 1995 Battlefield Environment Conference*, White Sands Missile Range, NM (December 1995).

5. Joel Mozer, Guy Seeley, Alan Wetmore, Patti Gillespie, David Ligon, and Samuel Crow, "Radiometric Validation of CSSM," *Proceedings of the 1997 CIDOS (Cloud Impacts on DOD Operations and Systems)*, Naval War College, Newport, RI (September 1997).

6. Alan Wetmore, Patti Gillespie, David Ligon, Michael Seablom, Samuel Crow, Guy Seeley, and Joel Mozer, "Experimental Evaluation of the Integrated WAVES-CSSM Model," *Proceedings of the 1997 Battlefield Atmospherics Conference*, San Diego, CA (December 1997).

7. Michael Rollins, *Evaluation of the Weather and Atmospheric Effects for Simulation (WAVES) Using Image Statistics*, STC technical report 6259, Science and Technology Corporation, Hampton, VA (1995).

8. T. B. McKee and S. K. Cox, "Scattering of Visible Radiation by Finite Clouds," *J. Atmos. Sci.* **31**, (1974), 1885–1892.

9. T. B. McKee and S. K. Cox, "Simulated Radiance Patterns for Finite Clouds," *J. Atmos. Sci.* **33** (1976), 2014-2020.

10. Andrew Zardecki, *Modification and Evaluation of the Weather and Atmospheric Visualization Effects for Simulation (WAVES) Suite of Codes*, Los Alamos Consulting report TCN-94-331 (June 1995).

11. Andrew Zardecki and Roger Davis, *Boundary Layer Illumination Radiation and Balance Model: BLIRB*, STC technical report 6211, final report under DAAD07-89-C-0035, Las Cruces, NM (April 1991).

12. Andrew Zardecki, *Three-Dimensional Extension of Boundary Layer Illumination Radiation Balance Model for Imaging Applications*, final report for DAAL03-91-C-0034, TCN 92-480, delivery order 0541 (December 1993).

13. David Tofsted and Sean O'Brien, *Three-Dimensional Radiative Transfer Modeling of Tropospheric Atmospheres*, U.S. Army Research Laboratory, ARL-TR-1629 (March 1998).

14. Michael B. Wells, *Monte Carlo Code for Evaluating the Boundary Layer Illumination and Radiation Balance Model BLIRB*, Wells Consulting report WCI-TR-9402 (September 1994).

15. Arnold Tunick, *The Refractive Index Structure Parameter/ Atmospheric Optical Turbulence Model: CN2*, U.S. Army Research Laboratory, ARL-TR-1615 (1998).

16. Michael Seablom, *WAVES Milestones and Evaluation Plan*, TASC/Litton white paper (1998).

17. Andrew Zardecki, *Validation of the Discrete Ordinates Method*, Interim report for DAALOS-91-C-0034 (1993).

Appendix. Model Suite Documentation Outline

The WAVES software is being documented through a series of Army Research Laboratory technical reports. The general volumes planned are outlined below, with short commentary on the contents of each volume.

Volume 1 **WAVES Overview**

This volume describes the general overview, capabilities, and philosophy behind the WAVES suite. It also summarizes the other documentation that is (or will be) available for WAVES.

Volume 2 **User's Guide**

This volume describes the use of the WAVES models and guides both the novice and experienced user through the many inputs and outputs of the various models.

Volume 3 **Sample Scenarios**

Sample scenarios are published in this volume, which may be updated periodically. These sample scenarios can be used to test the code for extreme conditions.

Volume 4 **BLIRB Technical Documentation**

The technical documentation describes the physics of the radiative transfer model in BLIRB, as well as the approximations and shortcomings of the model. This information can be found in Zardecki [3,10,12,17] and Zardecki and Davis [11].

Volume 5 **ATMOS Technical Documentation**

This report is technically very similar to the EOSAEL CN2MAR report published as part of the EOSAEL series of technical reports [15].

Volume 6 **3DSMOKE Technical Documentation**

The 3DSMOKE model is a direct adaptation of the EOSAEL COMBIC model combined with the STATBIC texture model to provide the inhomogeneous smokes.

Volume 7 **WAVES ToolKit**

This volume describes utilities built to assist in the use of WAVES. Utilities are important to the management of the information that must move between the various modules of WAVES [16].

Volume 8 **Model Evaluations**

This volume is a compilation of several model evaluations done on the models in WAVES and on WAVES as a suite of models. It may contain several subvolumes or parts. This information is already in several reports and papers (see Gillepsie et al [4], Mozer et al [5], Wells [1,2], Wetmore et al [6], and Zardecki [3,17]).

Distribution

Admnstr
Defns Techl Info Ctr
Attn DTIC-OCP
8725 John J Kingman Rd Ste 0944
FT Belvoir VA 22060-6218

Mil Asst for Env Sci Ofc of the Undersec of
Defns for Rsrch & Engrg R&AT E LS
Pentagon Rm 3D129
Washington DC 20301-3080

Ofc of the Dir Rsrch and Engrg
Attn R Menz
Pentagon Rm 3E1089
Washington DC 20301-3080

Ofc of the Secy of Defns
Attn ODDRE (R&AT)
Attn ODDRE (R&AT) S Gontarek
The Pentagon
Washington DC 20301-3080

OSD
Attn OUSD(A&T)/ODDR&E(R) R J Trew
Washington DC 20301-7100

AMCOM MRDEC
Attn AMSMI-RD W C McCorkle
Redstone Arsenal AL 35898-5240

ARL Chemical Biology Nuc Effects Div
Attn AMSRL-SL-CO
Aberdeen Proving Ground MD 21005-5423

Army Corps of Engrs Engr Topographics Lab
Attn CETEC-TR-G P F Krause
7701 Telegraph Rd
Alexandria VA 22315-3864

Army Dugway Proving Ground
Attn STEDP 3
Attn STEDP-MT-DA-L-3
Attn STEDP-MT-M Bowers
Dugway UT 84022-5000

Army Field Artillery School
Attn ATSF-TSM-TA
FT Sill OK 73503-5000

Army Infantry
Attn ATSH-CD-CS-OR E Dutoit
FT Benning GA 30905-5090

Army Materiel Sys Analysis Activity
Attn AMXSY-AT Campbell
Aberdeen Proving Ground MD 21005-5071

Army Rsrch Ofc
Attn AMXRO-GS Bach
PO Box 12211
Research Triangle Park NC 27709

Army Strat Defns Cmnd
Attn CSSD-SL-L Lilly
PO Box 1500
Huntsville AL 35807-3801

CECOM
Attn PM GPS COL S Young
FT Monmouth NJ 07703

Dir for MANPRINT
Ofc of the Deputy Chief of Staff for Prsnnl
Attn J Hiller
The Pentagon Rm 2C733
Washington DC 20301-0300

Kwajalein Missile Range
Attn Meteorologist in Charge
PO Box 57
APO San Francisco CA 96555

Natl Ground Intllgnc Ctr
Army Foreign Sci Tech Ctr
Attn CM
220 7th Stret NE
Charlottesville VA 22901-5396

Distribution (cont'd)

Natl Security Agency
Attn W21 Longbothum
9800 Savage Rd
FT George G Meade MD 20755-6000

Science & Technology
101 Research Dr
Hampton VA 23666-1340

US Army Armament Rsrch Dev & Engrg Ctr
Attn AMSTA-AR-TD M Fisette
Bldg 1
Picatinny Arsenal NJ 07806-5000

US Army Aviation and Missile Command
Attn AMSMI-RD-WS-PL G Lill Jr
Bldg 7804
Redstone Arsenal AL 35898-5000

US Army CRREL
Attn CEREL-GP R Detsch,
Attn SWOE G Koenig
Attn Roberts
72 Lyme Rd
Hanover NH 03755-1290

US Army Edgewood RDEC
Attn SCBRD-TD G Resnick
Aberdeen Proving Ground MD 21010-5423

US Army Info Sys Engrg Cmnd
Attn ASQB-OTD F Jenia
FT Huachuca AZ 85613-5300

US Army Natick RDEC Acting Techl Dir
Attn SSCNC-T P Brandler
Natick MA 01760-5002

US Army Nuclear & Chem Agency
Attn MONA-ZB
Bldg 2073
Springfield VA 22150-3198

US Army OEC
Attn CSTE-EFS
Park Center IV 4501 Ford Ave
Alexandria VA 22302-1458

Director
US Army Rsrch Ofc
4300 S Miami Blvd
Research Triangle Park NC 27709

US Army Simulation, Train, & Instrmntn Cmnd
Attn J Stahl
12350 Research Parkway
Orlando FL 32826-3726

US Army STRICOM
Attn AMCPM-WARSIM S Veautour
Attn AMCPM-WARSIM Williams
Attn AMCPM-WARSIM Lavin
Orlando FL 32826

US Army Tank-Automtv Cmnd Rsrch, Dev, & Engrg Ctr
Attn AMSTA-TA J Chapin
Warren MI 48397-5000

US Army Topo Engrg Ctr
Attn CETEC-ZC
FT Belvoir VA 22060-5546

US Army TRADOC Anlys Cmnd—WSMR
Attn ATRC-WSS-R
White Sands Missile Range NM 88002

US Army Train & Doctrine Cmnd Battle Lab Integration & Techl Dirctrt
Attn ATCD-B J A Klevecz
FT Monroe VA 23651-5850

US Army White Sands Missile Range
Attn STEWS-IM-IT Techl Lib Br
White Sands Missile Range NM 88002-5501

US Military Academy
Mathematical Sci Ctr of Excellence
Attn MDN-A MAJ M D Phillips
Dept of Mathematical Sci Thayer Hall
West Point NY 10996-1786

Distribution (cont'd)

US Army TRADOC
Attn ATRC-WEC D Dixon
White Sands Missile Range NM 88002-5501

USATRADOC
Attn ATCD-FA
FT Monroe VA 23651-5170

Nav Air War Cen Wpn Div
Attn CMD 420000D C0245 A Shlanta
1 Admin Cir
China Lake CA 93555-6001

Nav Air Warfare Ctr Training Sys Div
Attn Code 494 A Hutchinson
12350 Research Parkway
Orlando FL 32826

Nav Surface Warfare Ctr
Attn Code B07 J Pennella
17320 Dahlgren Rd Bldg 1470 Rm 1101
Dahlgren VA 22448-5100

Naval Surface Weapons Ctr
Attn Code G63
Dahlgren VA 22448-5000

AFCCC/DOC
Attn Glauber
151 Patton Ave Rm 120
Asheville NC 28801-5002

AFSPC/DRFN
Attn CAPT R Koon
150 Vandenberg Stret Ste 1105
Peterson AFB CO 80914-45900

Air Force
Attn Weather Techl Lib
151 Patton Ave Rm 120
Asheville NC 28801-5002

ASC OL/YUH
Attn JDAM-PIP LT V Jolley
102 W D Ave
Eglin AFB FL 32542

Phillips Laboratory
Attn AFRL-VSBE Chisholm
Attn PL/LYP
29 Randolph Rd
Hanscom AFB MA 01731-3010

SPAWARSYSCEN
Attn J H Richter
53560 Hull Street
San Diego CA 92152-5001

USAF Rome Lab Tech
Attn Corridor W Ste 262 RL SUL
26 Electr Pkwy Bldg 106
Griffiss AFB NY 13441-4514

DARPA
Attn B Kaspar
3701 N Fairfax Dr
Arlington VA 22203-1714

NASA Marshal Space Flt Ctr
Atmospheric Sciences Div
Attn E501 Fichtl
Huntsville AL 35802

NASA Spct Flt Ctr
Atmospheric Sciences Div
Attn Code ED 41 1
Huntsville AL 35812

NIST
Attn MS 847.5 M Weiss
325 Broadway
Boulder CO 80303

Ashtech Inc
Attn S Gourevitch
1177 Kifer Rd
Sunnyvale CA 94086

Dept of Commerce Ctr
Mountain Administration
Attn Spprt Ctr Library R51
325 S Broadway
Boulder CO 80303

Distribution (cont'd)

Gleason Research Associates
Attn J Manning
3315 Bob Wallace Ave, Ste 203
Huntsville AL 35805

Hicks & Associates, Inc
Attn G Singley III
1710 Goodrich Dr Ste 1300
McLean VA 22102

Natl Ctr for Atmospheric Research
Attn NCAR Library Serials
PO Box 3000
Boulder CO 80307-3000

NCSU
Attn J Davis
PO Box 8208
Raleigh NC 27650-8208

NTIA ITS S3
Attn H J Liebe
325 S Broadway
Boulder CO 80303

OL-A/AFCCC/MST
Attn G McWilliams
151 Patton St Rm 120
Asheville NC 28801-5002

Pacific Missile Test Ctr
Geophysics Div
Attn Code 3250
Point Mugu CA 93042-5000

Army Rsrch Lab
Attn AMSRL-IS-EW
White Sands Missile Range NM 88002-5501

US Army Rsrch Lab
Attn AMSRL-IS-EW D Hoock
Battlefield Envir Dir
White Sands Missile Range NM 88002-5001

US Army Rsrch Lab
Attn AMSRL-D R Whalin
Attn AMSRL-DD J Rocchio
Attn AMSRL-CI-LL Techl Lib (3 copies)
Attn AMSRL-CS-AS Mail & Records Mgmt
Attn AMSRL-CS-EA-TP Techl Pub (3 copies)
Attn AMSRL-D
Attn AMSRL-IS J D Gantt
Attn AMSRL-SE-EE P Gillespie (30 copies)
Attn AMSRL-SE-EE A Wetmore (25 copies)
Attn AMSRL-SE-EE D Ligon (25 copies)
Attn AMSRL-IS-ES
Attn AMSRL-SE-EE Z G Sztankay
Adelphi MD 20783-1197

REPORT DOCUMENTATION PAGE

Form Approved
OMB No. 0704-0188

1. AGENCY USE ONLY *(Leave blank)*	2. REPORT DATE	3. REPORT TYPE AND DATES COVERED
	March 1999	Summary, 1997 to 1998

4. TITLE AND SUBTITLE Comparison Study of the BLITS and BLIRB Radiative Transport Models

5. FUNDING NUMBERS

DA PR: B53A
PE: 61102A

6. AUTHOR(S) David A. Ligon, Alan Wetmore, and Patti Gillespie

7. PERFORMING ORGANIZATION NAME(S) AND ADDRESS(ES)

U.S. Army Research Laboratory
Attn: AMSRL-IS-EO
2800 Powder Mill Road
Adelphi, MD 20783-1197
email: dligon@arl.mil

8. PERFORMING ORGANIZATION REPORT NUMBER

ARL-TR-1721-8

9. SPONSORING/MONITORING AGENCY NAME(S) AND ADDRESS(ES)

U.S. Army Research Laboratory
2800 Powder Mill Road
Adelphi, MD 20783-1197

10. SPONSORING/MONITORING AGENCY REPORT NUMBER

11. SUPPLEMENTARY NOTES

ARL PR: 8FEJ60
AMS code: P611102.53A

12a. DISTRIBUTION/AVAILABILITY STATEMENT Approved for public release; distribution unlimited.

12b. DISTRIBUTION CODE

13. ABSTRACT *(Maximum 200 words)*

This report is one in a series of volumes that document the atmospheric environment visualization software WAVES (Weather and Atmospheric Visualization Effects for Simulation). Each Volume in the series describes an aspect of the series of models. This particular report gives a comparison of the surface-based radiative transport (RT) code Boundary Layer Illumination and Transmission for Simulation (BLITS) with the volumetric radiative transport code the Boundary Layer Illumination and Radiation Balance (BLIRB). This comparison is made using a simple three--dimensional (3-D) scenario that consists of a homogeneous cubical cloud filled with an aerosol described by the Deirmendjian type C.1 cloud phase function. Comparisons of the two RT models are made relative to results from two separate but consistent Monte Carlo models. For this simple scenario, BLIRB was determined to perform better than BLITS for the complete range of optical depths used. The BLITS model failed to accurately describe the radiant intensity of the scattering in the atmosphere at low optical depths.

14. SUBJECT TERMS	15. NUMBER OF PAGES
Radiative transfer, Monte Carlo, discrete ordinates model, illumination	37
	16. PRICE CODE

17. SECURITY CLASSIFICATION OF REPORT	18. SECURITY CLASSIFICATION OF THIS PAGE	19. SECURITY CLASSIFICATION OF ABSTRACT	20. LIMITATION OF ABSTRACT
Unclassified	Unclassified	Unclassified	SAR

NSN 7540-01-280-5500

Standard Form 298 (Rev. 2-89)
Prescribed by ANSI Std. Z39-18
298-102